A hydrophilic microenvironment required for the channel-independent insertase function of YidC

Naomi Shimokawa-Chiba[a], Kaoru Kumazaki[b], Tomoya Tsukazaki[c,d], Osamu Nureki[b], Koreaki Ito[a], Shinobu Chiba[a1]

[a]Faculty of Life Sciences, Kyoto Sangyo University, Motoyama, Kamigamo, Kita-ku, Kyoto 603-8555, Japan; [b]Department of Biological Sciences, Graduate School of Science, The University of Tokyo, 7-3-1 Hongo, Bunkyo-ku, Tokyo 113-0033, Japan; [c]Department of Systems Biology, Graduate School of Biological Sciences, Nara Institute of Science and Technology, 8916-5, Takayama-cho, Ikoma, Nara, 630-0192, Japan; [d]JST, PRESTO, 4-1-8 Honcho, Kawaguchi, Saitama, 332-0012, Japan.

Submitted to Proceedings of the National Academy of Sciences of the United States of America

The recently solved crystal structure of YidC suggests that it mediates membrane protein insertion by means of an intramembrane cavity rather than a transmembrane pore. This novel concept of protein translocation prompted us to characterize the native, membrane-integrated state of YidC with respect to the hydropathic nature of its transmembrane (TM) region. Here, we show that the cavity-forming region of SpoIIIJ, a YidC homolog, is indeed open to the aqueous milieu of the Bacillus subtilis cells and that the overall hydrophilicity of the cavity, along with the presence of an arginine residue on several alternative sites of the cavity surface, is functionally important. We propose that YidC functions as a proteinaceous amphiphile that interacts with newly synthesized membrane proteins and reduces energetic costs of their membrane traversal.

membrane protein insertion | MifM | SpoIIIJ | YidC

Introduction

Biogenesis of membrane proteins, a fundamental cellular process essential for all living organisms, includes insertion of a newly synthesized membrane protein into the membrane followed by its folding and assembly with other cellular components. In the Sec-dependent pathway in bacteria, membrane insertion is mediated by the SecYEG protein-conducting channel in the plasma (cytoplasmic) membrane (1-3) whereas acquisition of the native conformation is facilitated by the conserved YidC/Oxa1/Alb3 family of membrane proteins (4-7). In a Sec-independent pathway, YidC facilitates insertion of a class of membrane proteins independently of SecYEG. Thus, YidC is a dual-function protein that serves as a chaperone or an insertase in membrane protein biogenesis (4-7).

Bacillus subtilis possesses two YidC homologs, SpoIIIJ (YidC1) and YidC2 (YqjG). These proteins in combination with their substrate MifM have provided us a unique in vivo experimental system to study YidC. While SpoIIIJ and YidC2 share growth-essential functions, indicated from the synthetic lethal phenotype of their deletion (8, 9), SpoIIIJ is constitutively expressed and YidC2 is induced upon dysfunction of SpoIIIJ (10, 11) in a manner repressible autogenously (12). MifM is encoded from the upstream open reading frame of *yidC2* and plays an essential role in this cross-feedback and autogenous regulation by undergoing regulated elongation arrest in its translation (12-14). The ribosome stalling at *mifM* leads to exposure of the Shine-Dalgarno (SD) sequence of *yidC2* to enhance its translation. Importantly, elongation arrest of *mifM* is released upon the YidC-dependent membrane insertion of the nascent MifM polypeptide, enabling the *yidC2* translation to be up-regulated when cellular YidC activity declines. In this manner, MifM enables the cell to maintain the capacity of the YidC pathways of membrane protein biogenesis under changing intracellular and extracellular conditions (11, 12). This regulatory system also enables us to monitor the in vivo activities of YidC proteins; expression of a *yidC2'-lacZ* translational fusion gene and, hence, the β-galactosidase activity, will increase in response to a decrease in the SpoIIIJ activity (11).

Although both SecYEG and YidC could facilitate membrane protein insertion, their modes of actions are fundamentally different. For instance, while SecYEG can mediate membrane insertion of proteins with multiple TM segments as well as those having large extracytoplasmic (periplasmic) domains, YidC, as an insertase, is specialized in insertion of small membrane proteins that possess a single or two TM segment(s) and (a) short extracytoplasmic region(s) (7). Crystal structures of archaeal and bacterial SecYEβ and SecYE(G) complexes reveal an hourglass-shaped transmembrane pore formed by the TM segments of SecY. The pore can also open laterally to the lipid phase of the membrane, allowing release of a TM segment of substrates out of the translocon pore to establish membrane protein integration (15-17). Although earlier electronmicroscopic studies of *E. coli* YidC and *S. cerevisiae* Oxa1 led to a proposal that YidC forms a homo-dimer, which creates a channel-like structure at the subunit interface (18), more recent evidence suggests that a monomer of YidC interacts with the ribosome that is translating a membrane protein (19, 20). The crystal structures of YidC from *Bacillus halodurans* at resolution up to 2.4 Å (21) revealed that the five TM segments of YidC forms a cavity presumably in the lipid bilayer. This cavity appears to be open to the lipidic phase and the cytoplasm but not to the extracytoplasmic environment (Fig. 1A and B), arguing against the dimeric insertion pore model. Strikingly, the concave surface of the cavity is enriched in hydrophilic amino acid residues, including a conserved arginine. Genetic

Significance

How membrane proteins are guided into the membrane is a fundamental question of cell biology. Translocons are known to create a polypeptide-conducting, transmembrane channel having a lateral gate to allow lipid phase partitioning of the substrate. Here, we show that YidC guides a class of membrane proteins in a channel-independent fashion. Our experiments using intact Bacillus subtilis cells show that SpoIIIJ, a YidC homolog, forms a water-accessible cavity in the cell membrane and that the cavity's overall hydrophilicity as well as the presence of an arginine residue at one of several alternative places on the cavity is functionally important. Probably, extracellular part of substrate is first attracted to the YidC cavity before establishment of a transmembrane configuration through hydrophobic partitioning.

Reserved for Publication Footnotes

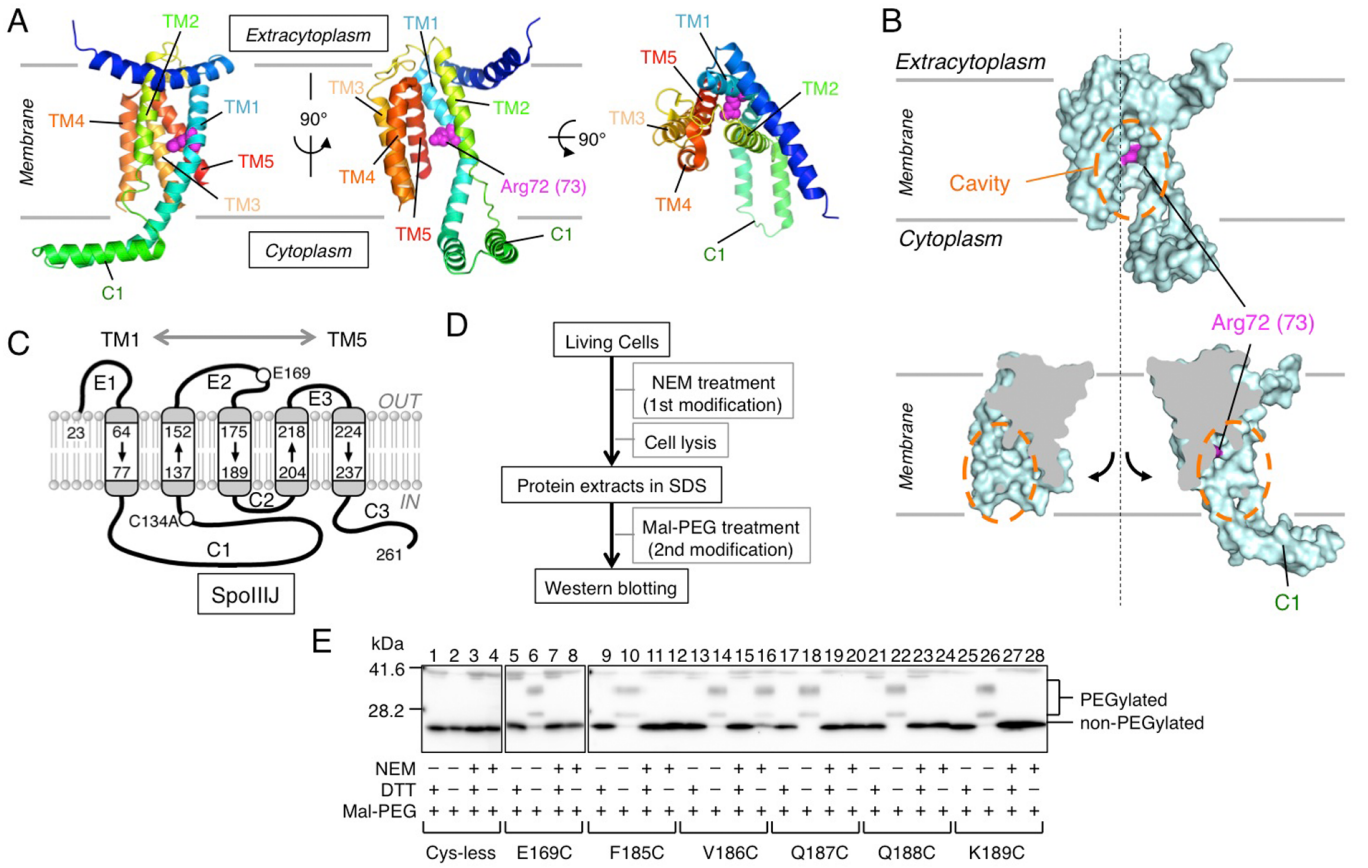

Fig. 1. . **Experimental design of NEM-reactivity assay to assess water accessibility to the SpoIIIJ cavity. (A)** Ribbon diagram representations of the crystal structure of *B. halodurans* YidC2 (PDB ID: 3WO6). Shown are the side views (left and center) and a top view (right). Arg72 (corresponding to Arg73 in *B. subtilis* SpoIIIJ; Fig. S1) is shown by magenta spheres. TM and C1 indicate the transmembrane segments (with numbers) and the first cytoplasmic region, respectively. **(B)** A surface model (upper) and cut-away molecular surface representation (lower) of *B. halodurans* YidC2. Orange dot-lined circles encircle the intramembrane cavity. Arg72 (Arg73 in SpoIIIJ) is shown in magenta. **(C)** A schematic representation of the membrane integration topology of *B. subtilis* SpoIIIJ and the sites where a unique cysteine was introduced for NEM-reactivity assay. TM1-TM5, C1-C3 and E1-E3 show the transmembrane, the cytoplasmic, and the extracytoplasmic regions, respectively. **(D)** The work flow of the assay. Intact cells were treated with NEM. Proteins were then extracted with SDS and subjected to PEGylation of the remaining thiols under denaturing conditions. Finally, SpoIIIJ species were visualized after SDS-PAGE. **(E)** Electrophoretic separation of the PEG-modified and unmodified SpoIIIJ species. Positions of cysteine introduced into SpoIIIJ are shown at the bottom. Each sample received four different treatments as indicated by + and –. DTT in excess was included in alternate samples at the PEGylation step to give unmodified controls. PEGylated SpoIIIJ forms multiple slow-migrating bands due to heterogeneity of the Mal-PEG preparation. The bands near the 42 kDa position are non-specific.

analyses of a *B. subtilis* YidC homolog, SpoIIIJ, and its substrate membrane protein, MifM, revealed that the positive charge of the conserved arginine (Arg73 in SpoIIIJ) as well as negatively charged residues in the extracytoplasmic and transmembrane regions of MifM are essential for insertion of MifM into the membrane (21). From these results we proposed that SpoIIIJ mediates insertion of a class of membrane proteins such as MifM by a channel-independent mechanism, in which electrostatic attraction between the SpoIIIJ cavity and the substrate initiates the reaction (21). The other *B. subtilis* YidC homolog, YidC2 (YqjG), also functions with similar mechanism for insertion of MifM (12). The importance of the cavity was also supported by photo-crosslinking experiments showing that the inner surface of the cavity of SpoIIIJ interacts with substrate protein in vivo (21). Together with the crystal structure of *Escherichia coli* YidC (22), it is suggested that having a hydrophilic and positively charged cavity is a feature shared by the YidC family members.

Since the unprecedented hydropathic arrangement of YidC bears crucial importance in our understanding of membrane protein biogenesis, its occurrence in the native membrane must be verified using intact living cells. Here, we explored the hydropathic nature and the functional requirements of the cavity-forming transmembrane region of SpoIIIJ in intact cells. The YidC cavity indeed proved to be accessible by water and its hydrophilicity, including an arginine residue somewhere in the cavity, important functionally. That YidC creates an aqueous microenvironment in the membrane gives a strong support to the channel-independent mode of its action.

Results

Water-accessibility of the SpoIIIJ intramembrane cavity

YidC forms an intramembrane cavity that is open laterally, presumably toward the lipid phase of the membrane and the cytoplasm, whereas it is inaccessible from the extracytoplasm (Fig. 1A and B). The inner surface of the cavity contains several hydrophilic amino acid residues, including the essential arginine, raising a possibility that YidC forms a hydrophilic local environment in the otherwise hydrophobic lipid bilayer. To experimentally verify this unusual hydropathic arrangement, we examined water accessibility of YidC TM residues using intact living cells and the NEM (N-ethylmaleimide)-reactivity assay. NEM is membrane-permeable and alkylates the thiol group of a cysteine residue of protein in a water-dependent reaction (23-25), enabling us to assess water availability of a specific site of the target protein in intact cells by strategically placing a cysteine residue.

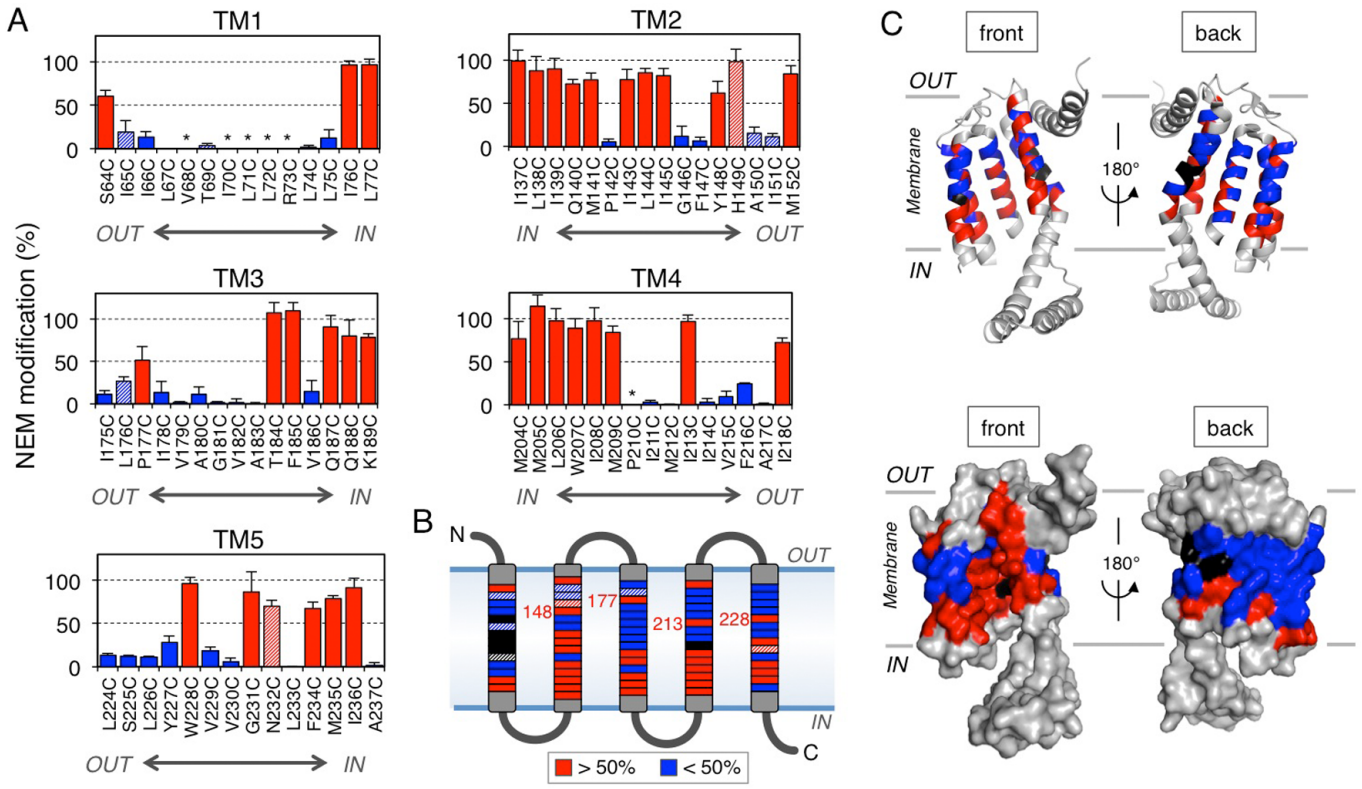

Fig. 2. Water accessibility profiles of the transmembrane regions of SpoIIIJ as assessed by NEM-reactivity. (A) NEM modification efficiencies (mean ± s.d., n ≥ 3) of cysteines at the indicated positions. Red columns show the efficiencies of > 50% and blue columns show lower (< 50%) modification efficiencies. Asterisks indicate SpoIIIJ derivatives that were unable to assess because of the lack of PEGylation even without NEM treatment. Striped columns represent non-functional SpoIIIJ mutants. **(B)** A schematic representation of the sites of cysteines and their NEM modification efficiencies. The sites of higher and lower modification as well as nonreactive sites are color-coded as in A. The numbered four positions are located in the extracytoplasmic half of the membrane but NEM-modified efficiently. The sites of non-functional cysteine substitutions are striped. **(C)** Ribbon (left) and surface (right) representations of the front and back views of the *B. halodurans* YidC2 structure with the color-coded water accessibility.

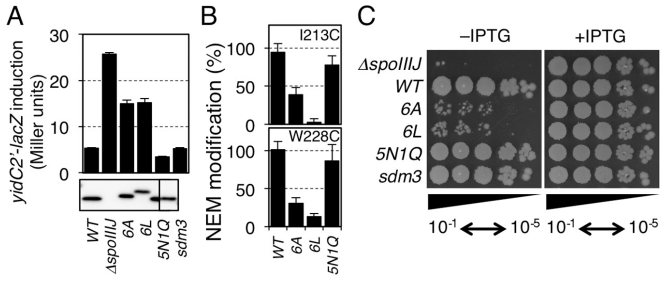

Fig. 3. Functional importance of hydrophilicity of the SpoIIIJ cavity. (A) Efficiencies of MifM insertion into the membrane by the SpoIIIJ variants. Upper panel shows β-galactosidase activities (mean ± s.d., n = 3) of the *spoIIIJ* mutant strains harboring the *yidC2*'-*lacZ* reporter gene, which inversely correlate with the efficiencies of MifM insertion. Lower panel shows cellular accumulation of SpoIIIJ derivatives determined by anti-SpoIIIJ immunoblotting. **(B)** NEM modification efficiencies of cysteine introduced either at the 213rd or 228th position of the wild type and SpoIIIJ cavity mutants indicated at the bottom. **(C)** Growth-supporting abilities of the SpoIIIJ cavity mutants. Complementation assay of *B. subtilis* was carried out using strains lacking the *yidC2* gene and having a rescue plasmid encoding IPTG-inducible *spoIIIJ*-FLAG. The chromosome contained the indicated *spoIIIJ* alleles shown on the left. Cultures were serially diluted (from 10^{-1} to 10^{-5}) and spotted onto LB agar plates containing 0 (right panel) or 1 mM (left panel) IPTG, which were then incubated for 17.5 hours at 37°C.

We first constructed the cysteine-less SpoIIIJ (SpoIIIJ-C134A), which proved to be functional as shown by the low β-galactosidase activity of the *yidC2*'-*lacZ* reporter (Fig S2), whose expression level inversely correlates with the efficiency of membrane insertion of MifM, a YidC substrate (11). We then introduced a cysteine residue into selected single positions of the cysteine-less SpoIIIJ. Mutant proteins were expressed from the native chromosomal locus under the control of the native *spoIIIJ* promoter. Intact cells were then treated with NEM directly without any cell disruption (Fig. 1D).

Proteins extracted from NEM-treated cells are solubilized, denatured in SDS and then subjected to the counter modification with maleimide-PEG (Mal-PEG), an alkylating reagent of ~5 kDa (Fig. 1D). An NEM-unmodified fraction of the target protein, still having free thiol, is now modified by Mal-PEG and mobility-shifted, whereas the NEM-modified fraction of the protein resists the counter modification and does not show any appreciable mobility shift. The efficiency of NEM-modification was assessed by the extent of counter modification with Mal-PEG (26).

To characterize this assay system, we first replaced Glu169 in the second extracytoplasmic (E2) loop with cysteine. SpoIIIJ-C134A/E169C thus constructed was expected to have a fully water-accessible cysteine (Fig 1C). When NEM was omitted from the first reaction, the protein was efficiently modified with Mal-PEG with concomitant disappearance of the unmodified species (Fig 1E, lane 6). The cysteine-less SpoIIIJ did not show this mobility shift and the intensity of the unmodified band remained unchanged (Fig. 1E, lanes 1-4). By contrast, NEM treatment of the E169C-expressing cells almost completely blocked the Mal-PEG modification even after denaturation (Fig. 1E, lane 8), indicating that the cysteine at this position was fully accessible by NEM and water as expected.

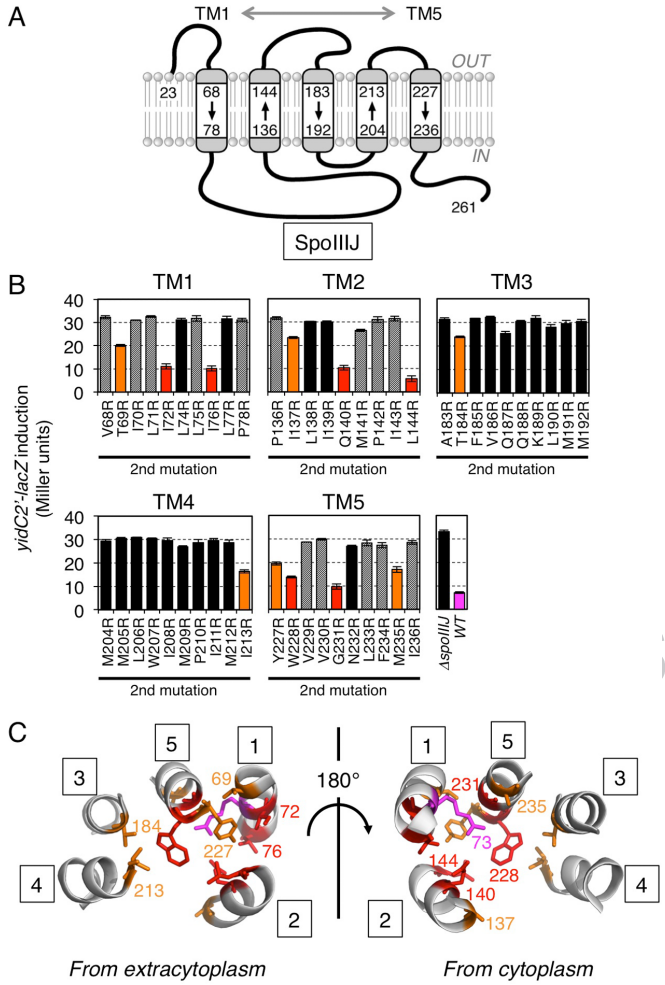

Fig. 4. Consequences of relocation of the essential arginine in SpoIIIJ. (A) The target boundary of arginine relocation experiments shown in the SpoIIIJ topology model. **(B)** Efficiencies of MifM insertion into the membrane by the SpoIIIJ variants. Reported are β-galactosidase activities (mean ± s.d., n = 3) of the *spoIIIJ* mutant strains harboring the *yidC2'-lacZ* reporter gene. All strains, except *ΔspoIIIJ* and wild type (WT), had the Arg73Ala mutation and an additional second site mutation indicated at the bottom in SpoIIIJ. Red, orange and black columns represent SpoIIIJ mutants with low (< 15 units), intermediate (15-25 units) and high (> 25 units) activities of β-galactosidase, indicative of high, intermediate and low efficiencies of MifM insertion, respectively. Mutant proteins that did not significantly accumulate in the cell are striped. β-galactosidase activity of wild type strain was shown in magenta. **(C)** Ribbon representations of the TM regions (numbered in squares) of *B. halodurans* YidC2 with the sites of functional Arg relocation (in SpoIIIJ) highlighted by side chains colored in red (high activity) and orange (intermediate activity). The *B. subtilis* numbering is used. The original Arg73 is shown in magenta.

We examined a total of 74 single-cysteine mutant derivatives of SpoIIIJ to cover the TM regions of SpoIIIJ (Fig. 1C). Images of immunoblotting in the NEM-reactivity assay are shown in Fig. 1E (lanes 9-28) for selected target positions and in Fig. S3 for all the positions examined. Cysteines at positions 185, 187, 188 and 189 were fully reactive with NEM, as judged from the lack of counter modification with Mal-PEG (Fig 1E, lanes 10 vs 12, lanes 18 vs 20, lanes 22 vs 24 and lanes 26 vs 28, respectively). By contrast, cysteine at position 186 was not markedly reactive with NEM, as judged from the evident counter modification (lanes 14 vs 16). These results suggest that water molecules can access residues 185, 187, 188 and 189 but not effectively residue 186. Average NEM modification efficiencies in at least three independent experiments, calculated as described in Experimental Procedures, are shown in Fig. 2A. The summarized water accessibility features are depicted in Fig. 2B and C (efficiently modified residues are shown in red). We note that cysteines at positions 68, 70, 71, 72, 73 and 210 (shown by asterisks in Fig 2A and in black in Fig 2B, C and Fig. S3) were not efficiently modified with Mal-PEG even without the first NEM modification. These positions may have been buried in a manner inaccessible by the alkylating agents and/or water, even after denaturation with SDS.

The results presented above show, strikingly, that numerous positions of the TM segments of SpoIIIJ are facing an aqueous environment. We note a tendency that the residues located closer to the cytoplasm exhibit higher modification efficiencies than those located in the distal side, with some exceptions (Fig 2 A-C). It is remarkable that the eight positions (S64, Y148, H149, M152, P177, I213, I218 and W228) are still highly accessible by water, even though they are located at the extracytoplasmic half of the bilayer membrane. Among these residues, S64, M152 and I218 are likely to be exposed to the extracytoplasmic environment, as shown from the crystal structure, explaining their high reactivity. By contrast, the other five NEM-modifiable residues in the distal half are likely embedded in the lipid bilayer, among which Y148, P177, I213 and W228 project their side chains toward the interior of the concave cavity.

In summary, our systematic in vivo NEM-modification assay suggests that the SpoIIIJ cavity creates an aqueous environment in the living cell membrane. Functional assays showed that most of the mutant SpoIIIJ derivatives were functional, although some others were less functional (Fig. S2). Although we included the non-functional SpoIIIJ mutants (Fig. S2 and those shown in striped colors in Fig. 2A and B) in our analysis, omitting them does not essentially affect our conclusion.

Functional importance of general hydrophilicity of the YidC cavity

We next addressed whether the hydrophilicity of the cavity is important for the YidC function. In our previous genetic studies, single alanine substitutions for the conserved hydrophilic residues in the cavity did not deteriorate SpoIIIJ functions, except for Arg73 (21). We reason that single alanine substitutions may be insufficient to reduce the overall hydrophilicity of the cavity. We therefore selected six hydrophilic residues in the cavity (Gln140, Thr184, Gln187, Gln188, Gly231, Asn232) that were efficiently modified by NEM (Fig. 2) for their simultaneous replacement with either alanine (SpoIIIJ-6A) or leucine (SpoIIIJ-6L) to make the cavity more hydrophobic. As a control, we constructed a mutant, in which the six residues were replaced either by hydrophilic asparagine or glutamine (SpoIIIJ-5N1Q, having mutations Q140N, T184N, Q187N, Q188N, G231N and N232Q). NEM-reactivity of cysteine introduced either at the 213th or the 228th position was significantly lowered by the *spoIIIJ-6A* and the *spoIIIJ-6L* mutations (Fig. 3B). By contrast, the NEM-reactivity remained unaffected at the high level by the *spoIIIJ-5N1Q* mutation.

We then assessed the insertase activity of the SpoIIIJ mutants using the *yidC2'-lacZ* reporter. Whereas cell expressing wild type *spoIIIJ* had a β-galactosidase activity of 5.3 units (Fig. 3A, column 1), the *spoIIIJ*-deletion strain (*ΔspoIIIJ*) had 25.7 units of it (Fig 3A, column 2). β-galactosidase activity of cells expressing *spoIIIJ-6A* was 15.0 units and that of *spoIIIJ-6L*-expressing cells was 15.2 units, showing defects in SpoIIIJ function. By contrast, cells expressing *spoIIIJ-5N1Q* had only 3.5 units, showing full functionality of SpoIIIJ. Immunoblotting showed that cellular abundance was similar for the SpoIIIJ variants examined, except for SpoIIIJ-6L, which was at a slightly lower level (Fig. 3A, lower panel). However, this slight decrease in the accumulation level does not explain the lower activity of SpoIIIJ-6L, since cells expressing wild type SpoIIIJ at a similarly decreased abundance due to a

mutation in the Shine-Dalgarno sequence (*sdm3-spoIIIJ*) showed the normal reporter expression (Fig. 3A, *sdm3*). Thus, the *spoIIIJ-6A* and the *spoIIIJ-6L* mutations impair the activity of SpoIIIJ to insert MifM into the membrane.

Deletion of *yidC2* makes *spoIIIJ* essential for cell viability (8, 9), allowing us to examine functionality of the SpoIIIJ mutant derivatives in supporting growth of *B. subtilis*. We used plasmid expressing *spoIIIJ-FLAG* under the IPTG-inducible promoter to assess the growth phenotypes of *spoIIIJ* mutations on the chromosome that was also deleted for *yidC2*; in the absence of IPTG the chromosomal *spoIIIJ* (with a mutation to be tested) was the sole source of YidC. We observed severe growth defects for strains having the *spoIIIJ-6A* or the *spoIIIJ-6L* mutation in the absence of IPTG. By contrast, the *spoIIIJ-5N1Q* and the sdm3-*spoIIIJ* cells grew normally even in the absence of IPTG. These results show that the hydrophilicity of the cavity is required for the growth-supporting function of SpoIIIJ. Taken together with the results obtained from the *lacZ* reporter assay, the SpoIIIJ cavity must be hydrophilic to function normally.

Flexible positional requirements for the essential positive charge within the YidC cavity

The SpoIIIJ cavity contains an arginine residue that is functionally essential, leading us to propose a charge attraction model for the initiation of translocation of MifM-like substrates (21). In this case, substrate recognition may not be based on strict structural complementarity and electrostatic interaction may allow certain positional flexibility. We addressed whether the arginine residue can be relocated to different positions on the cavity, by constructing a series of SpoIIIJ mutants with the original Arg73 replaced with alanine and having a unique arginine at various positions within the TM segments of SpoIIIJ. Western blotting experiments showed that the arginine-relocating mutations sometimes destabilized the SpoIIIJ protein (Fig. S4). Most of the unstable protein had an arginine residue outside the cavity (shown in blue in Fig. S4, A and B), which may have caused severe hydrophobic mismatches.

We used the *yidC2*'-*lacZ* reporter assay and the growth complementation assay to assess functionality of the mutant forms of SpoIIIJ. While many Arg-relocated mutants gave elevated β-galactosidase activity, comparable to the activity observed with the *spoIIIJ*-deleted cells (Fig 4B, mutants shown in black columns) as well as with cells carrying the *spoIIIJ-R73A* mutation (21), several mutants expressed β-galactosidase at levels significantly lower than the above-mentioned class of mutants. The latter SpoIIIJ variants can still support MifM insertion even though they have lost the crucial arginine at the original position and instead contain a relocated arginine at a different position (Fig. 4B). Six of them (termed Class I that includes I72R, I76R, Q140R, L144R, W228R and G231R; shown in red in Fig 4B and C) had β-galactosidase activities of lower than 15 units, indicative of nearly full functionality in inserting MifM into the membrane. Remaining five mutants (termed Class II that includes T69R, I137R, T184R, I213R and M235R) had β-galactosidase activities ranging from 15 to 25 units, indicative of partial functionality. The class I mutations were found only in TM1, TM2 and TM5, whereas the class II mutations were found in all the five TM segments. Locations of these residues on the crystal structure of *B. halodurans* YidC2, revealed that they, except I72, project their side chains toward the inside of the cavity (Fig. 4C). The side chain of I72 projects toward TM2 but still seems to be accessible from the cavity interior. TM2 and TM5 are both geometrically close to TM1, where Arg73 originally resided, possibly explaining why the class I mutations occurred only in TM1, TM2 and TM5.

Growth complementation assay showed that all the class I and the class II R73A/I213R mutations fully supported cell growth in the absence of YidC2. The class II mutations other than R73A/I213R resulted in poor growth (Fig. S5). Thus, the abilities of the SpoIIIJ variants to support cell growth correlated well with their insertase activities. These systematic analyses strongly support the idea that the concave surface of the cavity must be positively charged to maintain the SpoIIIJ activity but some flexibility is allowed about exact positions of the positive charge, being consistent with the charge attraction model.

Discussion

Translocation of hydrophilic regions of a newly synthesized polypeptide across the hydrophobic lipid bilayer is an energetically challenging process in the membrane protein insertion pathways. While the SecYEG translocon overcomes this difficulty by forming a polypeptide-conducting channel that sequesters a translocating polypeptide from the lipidic environment (15-17), several lines of evidence (19, 20, 27), most notably the crystal structure of *B. halodurans* YidC2 (21), suggest that YidC uses a channel-independent mechanism.

The results of our systematic NEM-probing analysis of the mono-cysteine derivatives of SpoIIIJ indicate that the SpoIIIJ cavity provides an aqueous environment within the membrane of living cells. Although cysteine substitution at certain positions, such as in the midst of consecutive hydrophobic residues, could itself have altered the local disposition of the polypeptide, we envisage that such cases were rare except for the non-functional mutations. The overall conclusion obtained from our in vivo analysis agrees well with the crystal structures of YidC as well as the results of molecular dynamics simulation of YidC, showing the presence of water molecules in the cavity (21). The hydrophilic residues on the concave surface of the cavity should contribute to maintaining the local aqueous environment as simultaneous substitution of non-polar alanine or leucine for the six selected hydrophilic residues on the cavity significantly reduced the efficiencies of NEM-modification of a cysteine introduced into the cavity. Importantly, SpoIIIJ's activities to insert MifM as well as to support cell growth are compromised significantly by the *spoIIIJ-6A* and the *spoIIIJ-6L* mutations, corroborating the physiological importance of the cavity hydrophilicity.

A role of the YidC cavity may be to provide a hydrophilic environment in the otherwise hydrophobic lipid bilayer, thereby reducing the energetic cost required for insertion of hydrophilic regions of substrate into the membrane en route to the trans-side. It is also conceivable that the hydrophobic mismatch at the protein-lipid interface could elicit local structural rearrangements of the lipid bilayer (28, 29) so as to affect substrate-membrane interactions and thereby facilitate membrane insertion. We speculate that the YidC cavity is designed not simply as a hydrophilic platform but to allow for the unusual arrangement of intramembrane aqueous space to be compatible with the thermodynamic principle. While it is unknown how this is accomplished, the notion is consistent with the observations that placement of an arginine residue is possible within the cavity but not its outer regions without severely destabilizing the protein (Fig S4).

The functional arginine does not strictly require a unique positioning in the cavity, as we were able to relocate it from the original 73rd position to several other positions within the cavity without loss of function. Such positional flexibility appears to be consistent with the electrostatic attracting force serving as a primary driving force for insertion of substrate. As discussed previously, the cytosolic C1 region with hairpin-like helices may provide a substrate entry point (21). Therefore, arginines that are closer to the C1 region may have higher functionality as an insertase element, although such a positioning should also be compatible with the subsequent step of translocation completion.

The hydrophilic surface within the membrane interior might be also important for the chaperone functions of YidC in the Sec-dependent insertion pathway. For instance, transmembrane regions of membrane proteins may contain functionally impor-

tant polar residues, which might be unstable in the lipidic environment upon release from translocon until assembling with a partner transmembrane polypeptide also containing complementary polar residues (30, 31). It is tempting to speculate that the hydrophilic cavity of YidC provides a transient docking surface that binds a newly inserted TM segment before it finds a partner of assembly, like regular aqueous phase chaperones do in the inverted ways.

The YidC family contains divergent members in different organisms, which differ in the modes of cooperation with other factors including the signal recognition particle and the ribosome (32-35). Moreover, each homolog can have multiple functions and reaction mechanisms (7, 36-38). We envision that the peculiarity of having a hydrophilic cavity in the membrane may be a common feature conserved in many of the family members. Still, it is possible that the hydrophilic local environment is used differently in different YidC homologs. For instance, the cavity arginine in the *E. coli* YidC was reported to be dispensable for the insertase activity for the Pf3 coat protein, which requires the arginine when handled by *Streptococcus mutans* YidC2 (39). Further studies on this interesting membrane protein will advance our understanding of how living organisms manage to solve problems associated with the movement of macromolecules across hydropathic borders.

Experimental Procedures

Bacterial strains and plasmids

The *B. subtilis* strains and plasmids used in this study are listed in Table S1 and S3, respectively. Construction procedures of *B. subtilis* strains were summarized in Table S2 and described in Supporting Information.

Media and conditions for growth of *B. subtilis*

B. subtilis cells were cultured at 37°C in LB medium containing (an) appropriate antibiotic(s). Samples were withdrawn from 3-ml cultures at an absorbance at 600 nm (OD_{600}) of 0.5 to 1.0 for NEM-reactivity assay, β-galactosidase assay or Western blotting. Growth condition for the growth complementation assay was described in Supporting Information.

NEM-reactivity assay, β-galactosidase assay and Western blotting

NEM and Mal-PEG modifications were carried out as described in Supporting Information. Efficiency of NEM modification of SpoIIIJ was calculated by the equation: NEM modification (%) = 100 x (a – b)/a (26), where a is the PEGylation efficiency obtained without the NEM treatment of the cell and b is the PEGylation efficiency obtained from NEM-treated cells. The PEGylation efficiency (%) was calculated by the formula: 100 x (i_0-i)/i_0, in which i_0 and i represent intensity of SpoIIIJ at the non-PEGylated position, the former before PEGylation and the latter after PEGylation. We used the decrease in the band intensity of non-PEGylated species after Mal-PEG treatment (without taking the band intensity of the PEGylated species into account) because the PEGylated proteins were heterogeneous in sizes and low in transfer efficiency upon blotting. β-galactosidase activity assays (10) and Western blotting (12) using anti-SpoIIIJ antiserum (21) were performed as described previously.

Acknowledgements.

We thank Chika Tsutsumi, Tomoe Takino and Sayuri Shikata for technical support and Akiko Nakashima for secretarial assistance. This work was supported by grants from MEXT and JSPS Grant-in-Aid for Scientific Research (Grant No. 26116008, 25291006 and 24657095 to SC, 20247020 to KI, 26119007 and 26291023 to TT and 24227004 to ON) as well as by Private University Strategic Research Foundation Support Program from MEXT (Grant No. S1219 to KI).

1. Pohlschroder M, Hartmann E, Hand NJ, Dilks K, & Haddad A (2005) Diversity and evolution of protein translocation. *Annu. Rev. Microbiol.* 59:91-111.
2. Park E & Rapoport TA (2012) Mechanisms of Sec61/SecY-mediated protein translocation across membranes. *Annu Rev Biophys* 41:21-40.
3. du Plessis DJ, Nouwen N, & Driessen AJ (2011) The Sec translocase. *Biochim. Biophys. Acta* 1808(3):851-865.
4. Dalbey RE, Wang P, & Kuhn A (2011) Assembly of bacterial inner membrane proteins. *Annu. Rev. Biochem.* 80:161-187.
5. Wang P & Dalbey RE (2011) Inserting membrane proteins: the YidC/Oxa1/Alb3 machinery in bacteria, mitochondria, and chloroplasts. *Biochim. Biophys. Acta* 1808(3):866-875.
6. Xie K & Dalbey RE (2008) Inserting proteins into the bacterial cytoplasmic membrane using the Sec and YidC translocases. *Nature reviews. Microbiology* 6(3):234-244.
7. Dalbey RE, Kuhn A, Zhu L, & Kiefer D (2014) The membrane insertase YidC. *Biochim. Biophys. Acta* 1843(8):1489-1496.
8. Murakami T, Haga K, Takeuchi M, & Sato T (2002) Analysis of the Bacillus subtilis spoIIIJ gene and its Paralogue gene, yqjG. *J. Bacteriol.* 184(7):1998-2004.
9. Tjalsma H, Bron S, & van Dijl JM (2003) Complementary impact of paralogous Oxa1-like proteins of Bacillus subtilis on post-translocational stages in protein secretion. *The Journal of biological chemistry* 278(18):15622-15632.
10. Rubio A, Jiang X, & Pogliano K (2005) Localization of translocation complex components in Bacillus subtilis: enrichment of the signal recognition particle receptor at early sporulation septa. *J. Bacteriol.* 187(14):5000-5002.
11. Chiba S, Lamsa A, & Pogliano K (2009) A ribosome-nascent chain sensor of membrane protein biogenesis in Bacillus subtilis. *The EMBO journal* 28(22):3461-3475.
12. Chiba S & Ito K (2014) MifM monitors total YidC activities of Bacillus subtilis including that of YidC2, the target of regulation. *J. Bacteriol.* 197(1):99-107.
13. Chiba S & Ito K (2012) Multisite ribosomal stalling: a unique mode of regulatory nascent chain action revealed for MifM. *Mol. Cell* 47(6):863-872.
14. Chiba S, *et al.* (2011) Recruitment of a species-specific translational arrest module to monitor different cellular processes. *Proc. Natl. Acad. Sci. U. S. A.* 108(15):6073-6078.
15. Van den Berg B, *et al.* (2004) X-ray structure of a protein-conducting channel. *Nature* 427(6969):36-44.
16. Tsukazaki T, *et al.* (2008) Conformational transition of Sec machinery inferred from bacterial SecYE structures. *Nature* 455(7215):988-991.
17. Zimmer J, Nam Y, & Rapoport TA (2008) Structure of a complex of the ATPase SecA and the protein-translocation channel. *Nature* 455(7215):936-943.
18. Kohler R, *et al.* (2009) YidC and Oxa1 form dimeric insertion pores on the translating ribosome. *Mol. Cell* 34(3):344-353.
19. Seitl I, Wickles S, Beckmann R, Kuhn A, & Kiefer D (2014) The C-terminal regions of YidC from Rhodopirellula baltica and Oceanicaulis alexandrii bind to ribosomes and partially substitute for SRP receptor function in Escherichia coli. *Mol. Microbiol.* 91(2):408-421.
20. Wickles S, *et al.* (2014) A structural model of the active ribosome-bound membrane protein insertase YidC. *Elife* 3:e03035.
21. Kumazaki K, *et al.* (2014) Structural basis of Sec-independent membrane protein insertion by YidC. *Nature* 509(7501):516-520.
22. Kumazaki K, *et al.* (2014) Crystal structure of Escherichia coli YidC, a membrane protein chaperone and insertase. *Sci Rep* 4:7299.
23. Kimura-Someya T, Iwaki S, & Yamaguchi A (1998) Site-directed chemical modification of cysteine-scanning mutants as to transmembrane segment II and its flanking regions of the Tn10-encoded metal-tetracycline/H+ antiporter reveals a transmembrane water-filled channel. *The Journal of biological chemistry* 273(49):32806-32811.
24. Kaback HR, *et al.* (2007) Site-directed alkylation and the alternating access model for LacY. *Proc. Natl. Acad. Sci. U. S. A.* 104(2):491-494.
25. Bogdanov M, Zhang W, Xie J, & Dowhan W (2005) Transmembrane protein topology mapping by the substituted cysteine accessibility method (SCAM(TM)): application to lipid-specific membrane protein topogenesis. *Methods* 36(2):148-171.
26. Maegawa S, Koide K, Ito K, & Akiyama Y (2007) The intramembrane active site of GlpG, an E. coli rhomboid protease, is accessible to water and hydrolyses an extramembrane peptide bond of substrates. *Mol. Microbiol.* 64(2):435-447.
27. Kedrov A, *et al.* (2013) Elucidating the native architecture of the YidC: ribosome complex. *J. Mol. Biol.* 425(22):4112-4124.
28. White SH (2007) Membrane protein insertion: the biology-physics nexus. *The Journal of general physiology* 129(5):363-369.
29. Contreras FX, Ernst AM, Wieland F, & Brugger B (2011) Specificity of intramembrane protein-lipid interactions. *Cold Spring Harb Perspect Biol* 3(6).
30. Saint-Georges Y, Hamel P, Lemaire C, & Dujardin G (2001) Role of positively charged transmembrane segments in the insertion and assembly of mitochondrial inner-membrane proteins. *Proc. Natl. Acad. Sci. U. S. A.* 98(24):13814-13819.
31. Price CE & Driessen AJ (2010) Conserved negative charges in the transmembrane segments of subunit K of the NADH:ubiquinone oxidoreductase determine its dependence on YidC for membrane insertion. *The Journal of biological chemistry* 285(6):3575-3581.
32. Funes S, *et al.* (2009) Independent gene duplications of the YidC/Oxa/Alb3 family enabled a specialized cotranslational function. *Proc. Natl. Acad. Sci. U. S. A.* 106(16):6656-6661.
33. Jia L, *et al.* (2003) Yeast Oxa1 interacts with mitochondrial ribosomes: the importance of the C-terminal region of Oxa1. *The EMBO journal* 22(24):6438-6447.
34. Szyrach G, Ott M, Bonnefoy N, Neupert W, & Herrmann JM (2003) Ribosome binding to the Oxa1 complex facilitates co-translational protein insertion in mitochondria. *The EMBO journal* 22(24):6448-6457.
35. Lewis NE, *et al.* (2010) A dynamic cpSRP43-Albino3 interaction mediates translocase regulation of chloroplast signal recognition particle (cpSRP)-targeting components. *The Journal of biological chemistry* 285(44):34220-34230.
36. Errington J, *et al.* (1992) Structure and function of the spoIIIJ gene of Bacillus subtilis: a vegetatively expressed gene that is essential for sigma G activity at an intermediate stage of sporulation. *J. Gen. Microbiol.* 138(12):2609-2618.
37. Saller MJ, *et al.* (2011) Bacillus subtilis YqjG is required for genetic competence development. *Proteomics* 11(2):270-282.
38. Gray AN, *et al.* (2011) Unbalanced charge distribution as a determinant for dependence of a subset of Escherichia coli membrane proteins on the membrane insertase YidC. *MBio* 2(6):e00238-11.
39. Chen Y, Soman R, Shanmugam SK, Kuhn A, & Dalbey RE (2014) The role of the strictly conserved positively charged residue differs among the Gram-positive, Gram-negative and chloroplast YidC homologs. *The Journal of biological chemistry* 289(51):35656-67 .